

Lightning performance analysis aimed at evaluating changes in the insulator strings of the 500 kV transmission line affected by extreme winds

G. R. Calzolari, C. R. Saldaña

Abstract— Two transmission lines belonging to Uruguay’s 500 kV electrical system have been tripped by protection systems several times since 2001 with unsuccessful reclosures. Therefore, there were serious load sheddings. After a preliminary analysis it was verified that the trip actions occurred under local strong storms, characterized by extreme wind velocities. As a result, the outer phase insulator I-string swing angle exceeded the maximum value specified in the line design. With the purpose of reducing the transmission line outages caused by this phenomenon, the following alternatives have been under consideration: a) redesign the yokes b) remove the inner grading ring of the outer phase insulator I-string c) remove two or three insulators of the outer phase I-string, which has 26 toughened glass insulators in total. An insulation coordination study of one of the transmission lines was conducted in order to evaluate the feasibility of alternative c). This paper focuses on the most important aspects of the lightning performance analysis carried out with ATP (Alternative Transients Program) in order to calculate the total lightning outage rate of the transmission line.

Keywords: extreme winds, I-string swing angle, lightning performance, ATP.

I. INTRODUCTION

TWO transmission lines belonging to Uruguay’s 500 kV electrical system, named Pal-MA and Pal-MB, length equal to 220 km, carry 75 percent of the total load demanded by Montevideo city, main load center. These transmission lines have been tripped, with unsuccessful reclosures, by protection systems, several times since 2001. As a result, there were serious load sheddings. A task force was created in order to investigate the reasons why these events happened, and come up with possible solutions. In line with this, line Pal-MB was first analyzed. The first study carried out was the verification of the dead time associated with the single phase auto-reclosure. It was concluded then that the dead time of 800 ms is enough to reach successful reclosures. After a preliminary analysis of the events it was verified that the trip actions occurred under local strong storms, characterized by extreme wind velocities. Due to the information provided by the fault-

locator, it was possible to inspect the towers affected by the faults. As a result of the inspection, some cavities at the body of the tower and a hole in the inner grading ring (corona shield) of the outer phase insulator I-string were observed, provoked by the arc discharge. Fig. 1 shows the result of one of the inspections conducted.



Fig. 1. I-string affected

It was concluded that I-string swing angle exceeded the maximum value specified in the line design, due to the presence of extreme winds. Therefore, the distance conductor-to-tower leg is less than the minimum clearance for power frequency voltage and a single phase-to-ground fault happened, thus leading to an unsuccessful single-phase reclosure.

A report from Universidad de la República, Montevideo, Uruguay, established that a “downburst phenomenon”, associated with severe storms, was the main cause of the events recorded. The IEC 60826 standard does not take into account very high wind speed but infrequent winds, such as typhoons, downburst and tornadoes. This may explain the difference between the design and the events recorded.

With the purpose of reducing the transmission line outages caused by this phenomenon, the following alternatives have been under consideration: a) redesign the yokes b) remove the inner grading ring of the outer phase insulator I-string c) remove two or three insulators of the outer phase I-string, which has a total of 26 toughened glass insulators.

An insulation coordination study of the Pal-MB transmission line was conducted in order to evaluate the feasibility of the: a) I-string made out of 24 toughened glass insulators b) I-string made out of 23 toughened glass insulators c) options a) and b) without inner grading ring.

C. Saldaña works in Power System Protection, UTE, Bvar. A. Saravia 4292, Montevideo 11700, Uruguay (e-mail of corresponding author: gracclau@adinet.com.uy).

G. Calzolari works in Projects and Studies, UTE, Paraguay 2431, Of 634, Montevideo 11800, Uruguay (e-mail: gcalzolari@ute.com.uy).

II. GLASS INSULATOR REMOVAL

The removal of a few glass insulators and the inner grading ring was considered with the purpose of reaching the minimum distance conductor-to-tower leg during the I-string swing for higher wind velocities.

The Critical Swing Angle (θ_c) is defined as the angle for which the distance conductor-to-tower leg is the minimum clearance (d) established by insulation design for power frequency voltage. Fig. 2-(a) shows the design values of $\theta_c = 60^\circ$ and $d = 1.2$ m.

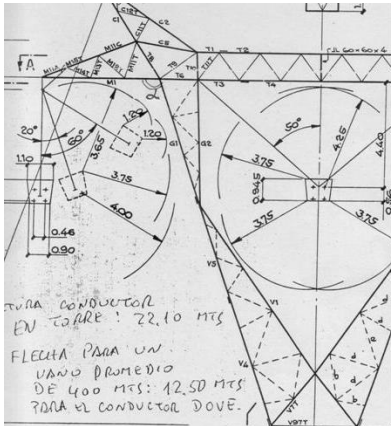


Fig. 2-(a) Tower top design

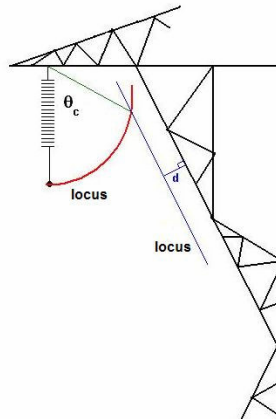


Fig. 2-(b) Critical Swing Angle

Fig. 2-(b) shows θ_c determined by the intersection of two loci: the circumference due to conductor motion and the straight line which keeps the minimum clearance (d).

Fig. 3 shows the I-string yoke with four bundle conductors and two grading rings. What must be analyzed here is which of the following points, A or B, has the lowest θ_c . In this case, point B has a critical swing angle equal to 59.7° , as shown in Fig. 3.

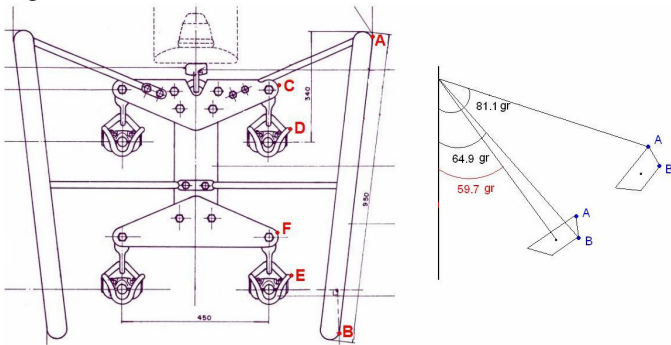


Fig. 3. Yoke and grading rings

Without the inner grading ring, what must be analyzed here is which of the points, C, D, E, F, has the lowest θ_c . In this case, point E has the lowest critical swing angle equal to 63.9° . The same procedure was repeated for the cases of I-string made out of 24 and 23 insulators. The overall results are shown in Table I. The swing angle equation described in [1] was utilized in order to calculate the wind velocities associated with critical swing angles. From the results presented in Table I, it can be concluded that: a) the critical swing angle increased

TABLE I

CRITICAL SWING ANGLES AND WIND VELOCITIES

Number of insulators	With inner grading ring		Without inner grading ring	
	Critical swing angle ($^\circ$)	Wind velocity (km/h)	Critical swing angle ($^\circ$)	Wind velocity (km/h)
26	59.7	176.1	63.9	191.2
24	63.1	187.7	68.1	210.9
23	65.1	196.3	70.6	225.1

by 9% and the wind velocity increased by 11.5% only removing three insulators. b) only removing the inner grading ring, the critical swing angle increased by 7% and the wind velocity increased by 8.6% c) the removal of both, three insulators and inner grading ring, increased the critical swing angle by 18.3% and the wind velocity by 27.8%.

These results encouraged the members in the task force to carry out an insulation coordination study of the line aimed at evaluating changes in the insulator I-strings.

III. INSULATION COORDINATION STUDY

The objective of an insulation design is to ensure that the insulation has enough strength to meet the stresses on it. Due to the various categories of voltage stresses three different types of line insulation design were conducted, considering the I-string made out of 26, 24 and 23 insulators with and without inner grading ring:

a) insulation for power frequency voltage. The analysis of the strength of the insulator I-string considered the determination of the minimum nominal specific creepage distance mm/kV and the pollution level. Standards IEC 60071-2 and IEC 815 were utilized. Also, the temporary overvoltages were taken into account through the calculation of the “earth fault factor”. The analysis of the strength of conductor-to-tower and conductor to grounded objects at midspan air-gaps were made by the AC flashover characteristics of a group of basic insulation configurations as reported by Aleksandrov [5].

b) insulation for switching surges. The problem of designing transmission line insulation for transient voltages is, as in most engineering problems, a balance between voltage stress and insulation strength. In relation to voltage stress IEC 60071-2 standard establishes that “the assumed maximum value of the representative overvoltage is equal to the truncation value of the overvoltages or equal to the switching impulse protective level of the surge arrester, whichever is the lower value”. For phase-to-earth overvoltage stress this standard recommends to assume the maximum value equal to the protective level of the surge arrester.

The I-string swing angle is equal to 20° for transient overvoltage insulation design. With reference to the insulator I-string strength determination, the procedure presented in Chapter 6 of [6] was adopted. Regarding conductor-to-tower and conductor-to-grounded objects at midspan air-gaps strength, the approach described in Chapter 11 of [5] was followed.

c) lightning performance. The most important aspects of the lightning performance analysis carried out are going to be presented in the following item.

IV. LIGHTNING PERFORMANCE ANALYSIS

There are three mechanisms through which lightning produces overvoltages on transmission lines: a) shielding failures, which involve flashes that bypass the overhead shield wires and terminate directly upon phase conductors. b) back-flashovers, which involve lightning strokes terminating on the shield wires near a tower. c) electromagnetic induction from nearby lightning flashes. These induced voltages are not a problem on EHV transmission lines.

The principal objective is the determination of the total transmission line outage rate caused by lightning disturbances, taking into account both the back-flashovers and shielding penetration flashovers. The total outage rate is the most probable number of line faults (tripouts) per 100 km per year. The calculation was carried out following two different approaches presented in [5], [6], [7], [8].

A. Edison Electric Institute approach

The Edison approach as described in Chapter 8, item 8.3, [6], allows for the calculation of the total line outage rate.

The following data were considered: a) isokeraunic level (I), 45 days/year b) number of insulators per string, 26, 24 and 23 c) shielding angle (θ), 20° d) tower height (h), 30.75m e) line standard span (S), 400m f) height of shield wires at midspan, 21m g) spacing between shield wires, 18.8m h) footing resistance, 10Ω i) height of conductor (y) at tower, 21.9m.

The total outage rate (T) is given by the following equation:

$$T = [1.65 * \beta * e^{\frac{-S}{2S_1}} * T' + F] * \frac{I}{100} \text{ per 100 miles per year (1)}$$

where: β per unit outage rate, S_1 span length of the base case, T' tripout rate of base case, F probability of shielding failure. The results are shown in Table II for different number of insulators.

TABLE II
TOTAL LINE OUTAGE RATE – EDISON

Number of insulators	T Tripouts/100 km.year	Pal-MB Line
26	0.15	1 outage every 3 years
24	0.205	1 outage every 27 months
23	0.205	1 outage every 27 months

The insulator removal increased the total outage rate by 36.7%.

B. Cigré, EPRI, IEEE approaches

The Cigré [7], EPRI [5] and IEEE [8] approaches were utilized in order to calculate the total line outage rate caused by direct lightning strokes and back-flashovers.

1) Direct Lightning Stroke

When a flash terminates directly on the phase conductor extremely high voltages will quickly develop at the contact point and then travel in both directions along the phase conductor, eventually reaching one or more gaps and causing a flashover. The insulator I-string and conductor-to-tower gaps were analyzed.

The shielding failure flashover rate (SFFOR) is defined by

the following equation [7]:

$$SFFOR = 2N_g L_1 \int_{I_c}^{I_m} D_c f(I) dI \text{ per 100 km per year (2)}$$

where: N_g ground flash density, L_1 line length, D_c exposure distance for a shielding failure, $f(I)$ probability density function of the stroke current, I_c minimum stroke current which causes a gap flashover, I_m maximum stroke current that can cause a shielding failure.

Fig. 4 shows the distance r_s , which is the strike distance corresponding to I_m current and which is determined by equation (3). The value obtained is 40.16m.

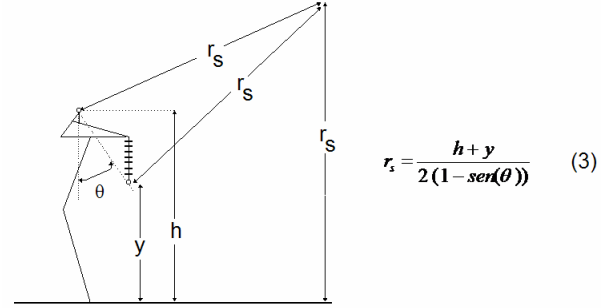


Fig. 4. Strike distance r_s

Knowing the r_s distance, the I_m values derived from the Electrogeometric Model are shown in Table III.

TABLE III
 I_m CURRENT

		I_m (kA)
IEEE	$r_s = 8(I)^{0.65}$	11.97
EPRI	$r_s = 10(I)^{0.65}$	8.5
CIGRE	$r_s = 7.1(I)^{0.75}$	10.08

With the aim of calculating the I_c current, the following equations were utilized:

$$I_c = \frac{2U_{50}}{Z_{phase}} \text{ (4) , } Z_{phase} = 60Ln\left(\frac{2H_m}{r}\right) \text{ (5)}$$

where: Z_{phase} phase conductor surge impedance (295.4Ω), r radius of the equivalent conductor, H_m average height of conductor, U_{50} critical flashover voltage.

Regarding the insulator I-string the flashover mechanism can be represented by volt-time curves, which in turn represent the relationship between the peak voltage of a specific impulse shape and the time to discharge. From the manufacturer's data and volt-time curve formulation [11] [8], similar U_{50} values were obtained. Values 2060 kV, 1918 kV and 1848 kV corresponding to 26, 24 and 23 toughened glass insulators, and given by the manufacturer, were chosen. Table IV shows the I_m and I_c values for different number of insulators.

TABLE IV
 I_m AND I_c VALUES INSULATOR I-STRING

I_m (kA)	Number of insulators	I_c (kA)
[11.97; 8.5; 10.08]	26	13.95
[11.97; 8.5; 10.08]	24	12.98
[11.97; 8.5; 10.08]	23	12.51

From the comparison of the values it can be concluded then that there are no flashovers for the insulator I-string gap made

out of 24 or 23 insulators.

With reference to the conductor-to-tower gap strength, the curves for rod-to-rod and rod-to-plane gaps, as described in Chapter 8 of [6], and which represent the relationship between the impulse critical flashover voltage and the gap spacing were utilized. The gap spacing was calculated with the inner grading ring in one instance and without it in another. It was calculated considering a swing angle equal to 20°, and different number of insulators. Table V shows the I_m and I_c values for all the cases.

TABLE V
 I_m AND I_c VALUES AIR GAP

I_m (kA)	Number of insulators	I_c (kA) With inner grading ring	I_c (kA) Without inner grading ring
[11.97; 8.5; 10.08]	26	13.54	> 13.54
[11.97; 8.5; 10.08]	24	11.85	12.86
[11.97; 8.5; 10.08]	23	11.08	11.85

From the comparison of the results it can be concluded then that with the EPRI and Cigre I_m values there are no flashovers in all the cases. Considering the IEEE I_m value: a) 24 insulators with inner grading ring present a SFFOR equal to 0.004291 /100km.year b) 23 insulators with inner grading ring present a SFFOR equal to 0.02993 /100km.year c) 23 insulators without inner grading ring present the same SFFOR as case a).

2) Back-flashover

A lightning stroke terminating on the shield wire, as shown in Fig. 5, creates waves of current and voltage which travel along the shield wire. At the tower, or at any point of impedance discontinuity, these waves are reflected back and are transmitted down the tower and outward on the shield wire to an adjacent tower. Due to capacitive coupling, current and voltage waves are induced on the phase conductors.

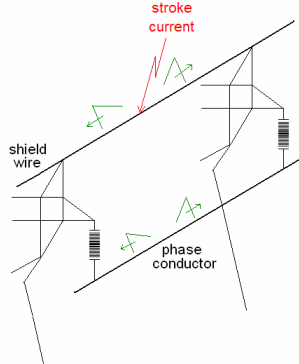


Fig. 5. Traveling waves

As a result, voltages are produced across the air and insulator I-string gaps. If one of the potentials exceeds the gap strength, flashover occurs. This event is called “back-flashover”.

The back-flashover rate (BFR) is defined by the following equation [7]:

$$BFR = 0.6N_L \int_{I_c}^{\infty} f(I) dI = 0.6N_L P(I_c) \quad \text{per 100 km per year} \quad (6)$$

where: $0.6N_L$ is the number of flashes to a tower per 100 km per year, $P(I)$ is the probability that the peak current in any

flash will exceed I_c . In order to calculate the I_c current, digital simulations were carried out with the ATP program. Regarding N_L value there are two formulations derived by EPRI and Cigré. The highest value equal to 100, from Cigré, was chosen as a worst case.

a) ATP modeling

The most important aspects of the ATP modeling are going to be presented.

The phase conductors and two shield wires were modeled through the untransposed distributed parameters line model calculated at 400 kHz. Four line spans were modeled at both sides of the struck tower. The line extended beyond the last tower can be represented by a characteristic impedance matrix.

The steel towers were represented as a single conductor distributed parameter line terminated by a resistance representing the tower footing impedance. The surge impedance of the tower (129.83 Ω) was calculated according to the formula outlined in [5], and the velocity of propagation was assumed to be equal to the speed of light. The footing resistance was chosen as a constant value 10 Ω at 50 Hz, adopting a conservative criterion. Fig. 6 shows one section of the equivalent circuit utilized for the studies.

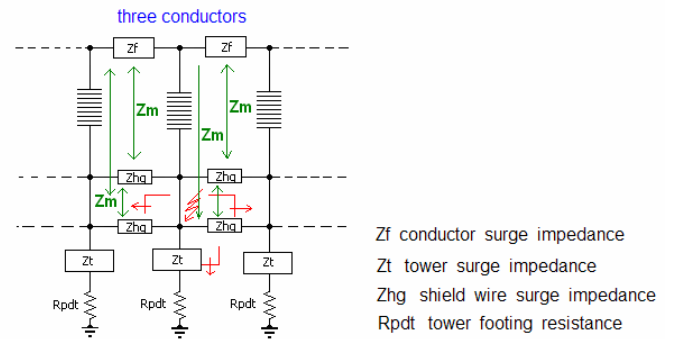


Fig. 6. Equivalent circuit

The stroke current wave-shape was approximated by a ramp function [5], [7]. The source type 12 of ATP was chosen for this modeling, which provides for a linear rise from zero to crest value. The ramp wave-shape parameters were selected according to a relationship between crest current, frontal rate of rise and time to crest, presented in [5].

The effect of the ac steady state voltage on a lightning surge was taken into account through an average value of power frequency voltage, as recommended in [7]. For a single-circuit horizontally-configured line, the mean value is 0.827 times the crest line-to-neutral voltage (355.8 kV).

b) I_c calculation by volt-time curves

The volt-time curves give the performance of insulation under the stress of the standard lightning impulse [5], [8], [11]. If the voltage developed across the air or insulator I-string gap touches the volt-time curve, a back-flashover occurs. The I_c calculation was made following these steps: 1) for a given insulator I-string and swing angle of 20°, the I-string and conductor-to-tower gap lengths were calculated 2) for each gap length a particular volt-time curve was determined from its experimental equation 3) the crest value of the stroke current and time to crest were varied until the voltage developed

across the gap touched the volt-time curve. This is the value of I_c . 4) the BFR was calculated through (6). This procedure was followed for the I-string made out of 26, 24 and 23 glass insulators with inner grading ring.

As an example, in the case of 24 glass insulators the I-string and air gap lengths are equal to 3.5 m and 3.19 m respectively. Fig. 7 and Fig. 8 show the volt-time curves and voltages developed across the gaps which caused back-flashover.

The I_c values corresponding to the I-string is 200 kA with $P(I_c)=0.78\%$ and to the air gap is 180 kA with $P(I_c)=1.02\%$.

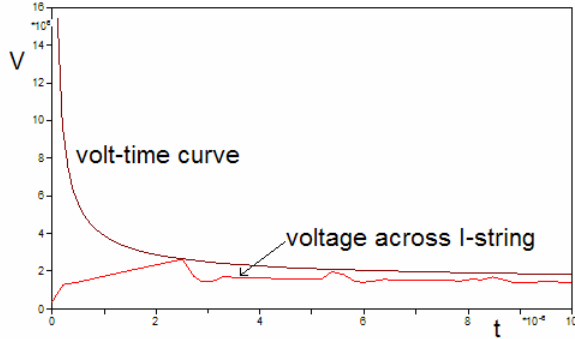


Fig. 7. I-string back-flashover (24 glass insulators)

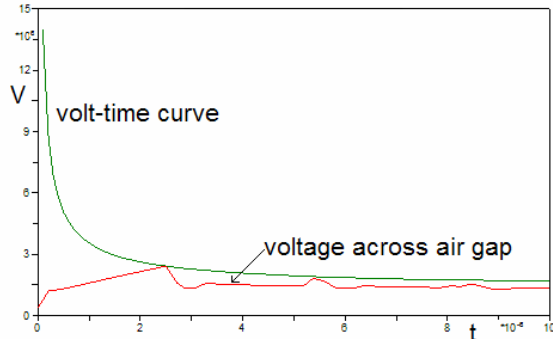


Fig. 8. Air gap back-flashover (24 glass insulators)

Table VI shows the BFR values for all the cases.

TABLE VI
BFR VALUES I-STRING AND AIR GAPS – VOLT-TIME CURVE

Number of insulators	BFR I-string gap	BFR air gap
26	0.342	0.414
24	0.468	0.612
23	0.534	0.708

c) I_c calculation by Leader Development Method

The Leader Development Method (LDM) takes into account physical aspects associated with the discharge mechanism [7], [8], [9]. The LDM is based on experimental results which in turn lead to the following differential equation:

$$\frac{dL}{dt} = KV(t) \left[\frac{V(t)}{g-L} - E_0 \right] \quad (7)$$

where: L leader length, m, V(t) voltage across gap, kV, g gap length, m, K and E_0 parameters depend on the gap configuration and the impulse polarity. The breakdown occurs when the leader length is equal to the gap length.

The LDM can be applied to a wide range of gap geometries, any impulse voltage polarity, any impulse voltage

waveform, and a gap length up to 7 m. Equation (7) was solved numerically by the Fourth-order Runge-Kutta method, and implemented in routine TACS of ATP using device Type-69.

The I_c calculation was carried out following these steps: 1) for a given insulator I-string and swing angle of 20° , the I-string and conductor-to-tower gap lengths were calculated 2) for each gap the crest value of the stroke current and time to crest were varied until the solution of (7) was equal to the gap length. This is the value of I_c . 3) the BFR was calculated through (6). This procedure was applied for the cases of 26, 24 and 23 glass insulators with inner grading ring.

As an example, for the case of 24 glass insulators Fig. 9 and Fig. 10 show the voltages developed across the gaps and the leader lengths development.

The I_c value corresponding to the I-string is 225 kA with $P(I_c)=0.57\%$ and the value to the air gap is 230 kA with $P(I_c)=0.54\%$.

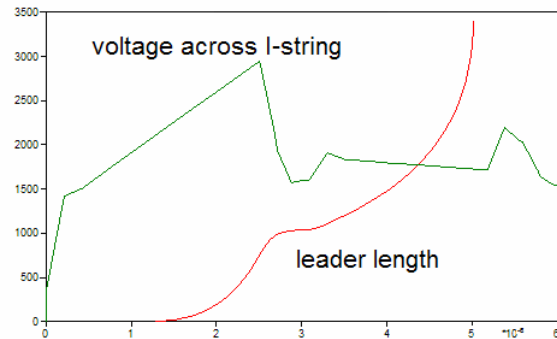


Fig. 9. LDM_ I-string back-flashover (24 glass insulators)

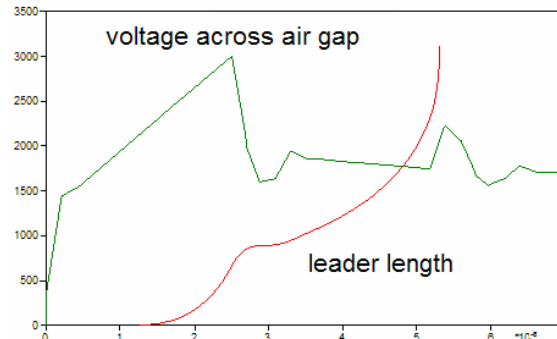


Fig. 10. LDM_ Air gap back-flashover (24 glass insulators)

Table VII shows the BFR values for all the cases.

TABLE VII
BFR VALUES I-STRING AND AIR GAPS - LDM

Number of insulators	BFR I-string gap	BFR air gap
26	0.276	0.216
24	0.342	0.324
23	0.390	0.366

d) Selection of the BFR values

From the results obtained by volt-time curves procedure we can conclude that the higher BFR values are caused by the air gap. The results obtained by the LDM procedure support the conclusion that the higher BFR values are caused by I-string

gap. All the results gotten with LDM method are less than those obtained with volt-time curves.

The differences pointed out above might be explained by the fact that the voltage wave shapes developed across the air, and insulator I-string gaps calculated with ATP are not standard impulses as required by volt-time curve procedure.

Therefore, we selected the BFR values derived by LDM method.

3) Total Line Outage Rate

The total line outage rate (T) is given by the sum of SFFOR and BFR rates. Table VIII shows the T values for different number of insulators.

TABLE VIII
TOTAL LINE OUTAGE RATE – CIGRE, EPRI, IEEE

Number of insulators	T Trips/100 km.year	Pal-MB Line
26	0.276 /100 km.year	1 outage every 20 months
24	0.342 /100 km.year	1 outage every 16 months
23	0.390 /100 km.year	1 outage every 14 months

V. CONCLUSIONS

The alternative of removal of two or three glass insulators of the outer phase I-string led to an insulation coordination study. From the results of the lightning performance analysis presented above we can conclude that:

a) SFFOR. The Cigré and EPRI values of I_m led to a shielding failure flashover rate equal to zero, which means “perfect shielding”. The IEEE value of I_m in the worst case increased the SFFOR in one outage every 15 years.

b) BFR. The LDM results show that the removal of two insulators increased the BFR by 23.9% and the removal of three insulators increased the BFR by 41.3%.

c) Total line outage rate. From the comparison of the values shown in Tables II and VIII, it could be observed that the Edison approach gives more optimistic results.

Taking into account these results, we can draw the conclusion that the removal of two or three insulators can be feasible from the lightning performance point of view.

From the power frequency voltage performance analysis carried out it can be concluded that:

a) the creepage distances corresponding to the I-string made out of 24 and 23 glass insulators comply with standard IEC 815, but do not comply with standard IEC 60071-2.

b) the line under study has been in service for 30 years. Some task force members are in charge of the maintenance of 500 kV lines and from their experience the removal of two or three insulators might be possible.

From the switching surges performance analysis done, the results support the conclusion that:

a) the removal of two or three insulators decreased the conductor-to-tower gap length, as well as the gap strength.

b) the results show that for 24 and 23 glass insulators with and without inner grading ring, the conductor-to-tower gap strength is less than the protective levels of the surge arresters.

Therefore, this is a serious constraint that makes impossible the alternative of removal of two or three insulators.

As mentioned in the Introduction of this paper, another alternative investigated was the redesign of some outer phase insulator I-string yokes. This was necessary due to the fact that the towers affected by the faults presented a ratio of weight span to wind span lower than 0.9 design value. For the same wind velocity these I-strings present a greater swing angle, and as a consequence, they are more prone to faults. The yoke redesign consisted of adding six plates to it in order to increase the ratio mentioned above, Fig. 11 shows the redesigned yoke. These plates were installed in a total of 72 towers with a successful operation up to now.

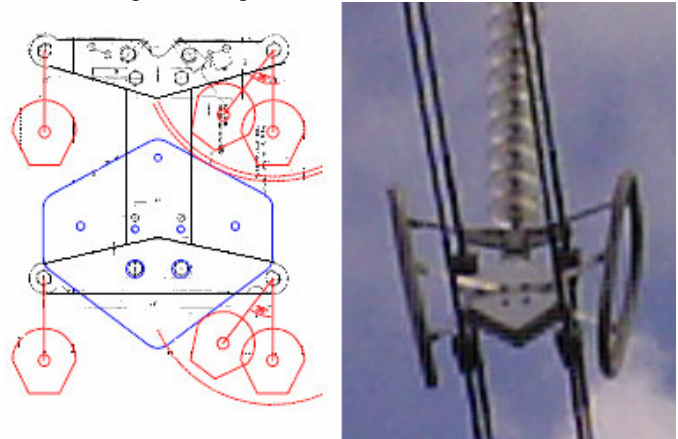


Fig. 11. Redesigned yoke

VI. REFERENCES

- [1] A. D’Ajuz et alli, *Transitorios Eléctricos e Coordenacao de Isolamento*, Rio de Janeiro: Furnas, 1987.
- [2] Working Group 22.06, "Tower Top Geometry," Cigré, Tech. Rep. 48, Jun. 1995.
- [3] *IEC Insulation Coordination*, IEC Standard 60071-1, 60071-2, 1993.
- [4] *IEC Design criteria of overhead transmission lines*, IEC Standard 60826, 2003.
- [5] *Transmission Line Reference Book – 345 kV and Above*, Palo Alto: Electric Power Research Institute, 1982.
- [6] *EHV Transmission Line Reference Book*, New York: Edison Electric Institute, 1968.
- [7] Working Group 01, "Guide to Procedures for Estimating the Lightning Performance of Transmission Lines," Cigré, Tech. Rep. 63, Oct. 1991.
- [8] A. F. Imece et alli, "Modeling Guidelines for Fast Front Transients," *IEEE Trans. Power Delivery*, vol. 11, pp. 493-501, Jan. 1996.
- [9] T. Shindo and T. Suzuki, "A New Calculation Method of Breakdown Voltage-Time Characteristics of Long Air Gaps," *IEEE Trans. Power Apparatus and Systems*, vol. PAS-104, N°6 pp. 1556-1563, Jun. 1985.
- [10] A. Ametani and T. Kawamura, "A Method of a Lightning Surge Analysis Recommended in Japan Using EMTP," *IEEE Trans. Power Delivery*, vol. 20, N°2 pp. 867-875, Apr. 2005.
- [11] J. R. Fonseca et alli, "Lightning Impulse Tests on Tower Models" *IEEE Trans. Power Apparatus and Systems*, vol. PAS-103, N°4 pp. 893-896, Apr. 1984.
- [12] "Alternative Transients Program (ATP)-RuleBook", Canadian/American EMTP User Group, 1987-92.